THE JOURNAL OF PHYSICAL CHEMISTRY B

 VOLUME 106, NUMBER 39, OCTOBER 3, 2002

LETTERS

Sulfonic Acid-Functionalized Mesoporous Silica: Synthesis, Characterization, and Catalytic Reaction of Alcohol Coupling to Ethers

James G. C. Shen, Richard G. Herman, and Kamil Klier*

Department of Chemistry and Zettlemoyer Center for Surface Studies, 6 East Packer Avenue, Lehigh University, Bethlehem, Pennsylvania 18015

Received: January 16, 2002; In Final Form: June 11, 2002

A propanesulfonic acid-derivatized mesoporous SBA-15 catalyst was synthesized, characterized in terms of surface properties, and shown to have high selectivities for alcohol coupling to form ethers, specifically from methanol and isobutanol coupling to form methyl isobutyl ether with no detectable formation of butenes at temperatures <400 K. Kinetic analysis was consistent with competitive adsorption of the two alcohols onto Brønsted acid sites, with isobutanol being more strongly adsorbed on the acid sites than the methanol.

The large number of aluminosilicate zeolites now available provides for a variety of novel and selective catalytic reactions, and much recent research has focused on the properties and application of these zeolitic materials. This recent research includes sorption[1] and phase transitions[2] in confined spaces, ion exchange,[3] preparation of intrachannel transition-metal catalysts,[3−5] and intraporous catalysis.[6] For example, CO hydrogenation and CH_4 homologation were performed on zeolitic transition-metal clusters, where the combination of intra-void metal and zeolite structure enhanced catalytic activity and selectivity of the desirable products.[7] However, complex cages and narrow channels in faujasite prevented the formation of branch-chain hydrocarbons/oxygenates in the CO/CH_4 hydrogenation. Sun et al.[8] reported alcohol coupling to form unsymmetrical ethers inside HZSM-5, where the cross coupling of ethanol and pentan-2-ol could not proceed inside either straight-type channels or elliptical-type channels but did proceed in the large space at the intersection of the channels. The result is consistent with inference that the narrow channels of ZSM-5 did not allow the ethanol to attack the pentan-2-ol adsorbed at internal Brønsted acid sites but only at the channel intersections, where the attack was from the rear end of the asymmetric carbon via a S_N2 reaction pathway to yield a chirally inverted ether.[8]

From a practical viewpoint, improvement of the ether yields from alcohol coupling over high surface area catalysts with a high concentration of acid sites was found to be desirable.[9,10] Further, kinetic analyses and theoretical calculations suggest that the catalytic mechanism of alcohol coupling is a S_N2 pathway involving competitive adsorption of reactants on proximal Brønsted acid sites.[9,10] Thus, a large-pore silica with internal strong acid species, high surface area, large void space, and thermal stability is expected to effectively catalyze ether formation. During the past decade, high surface mesoporous and relatively high thermal stability silica materials have been successfully synthesized.[11−13] These materials have recently been derived with strong acid species by covalent attachment of alkanesulfonic acid groups to the silica cavities.[14] To increase the concentration of the strong acid species, a direct synthesis method was used to synthesize periodic ordered sulfonic acid-functionalized mesoporous silica.[13a] This involves a one-step synthetic strategy based on the hydrolysis followed by co-condensation of tetraethoxysilane (TEOS) and (3-mercatopropyl)trimethoxysilane (MPTMS) under the templating of Pluronic 123 copolymer and in situ oxidation of thiol groups by H_2O_2 in aqueous acidic solution. The synthesis technique has now been employed to form a strong acid catalyst that is selective in the formation of unsymmetric ethers, i.e., the high cetane methyl

* Corresponding author. E-mail: kk04@lehigh.edu.

10.1021/jp020131h CCC: $22.00
Published on Web 09/05/2002

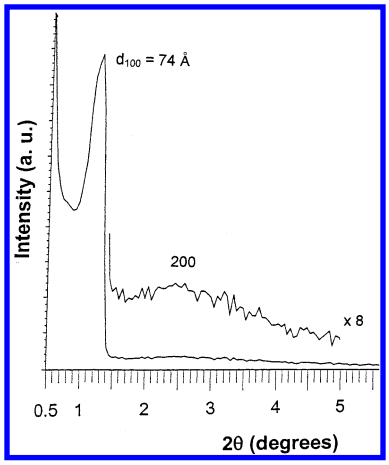

Figure 1. X-ray powder diffraction pattern of the extracted propanesulfonic acid-derivatized SBA-15 material.

isobutyl ether, from alcohols at moderate temperatures and ambient pressure.

A 4 g portion of Pluronic 123 (poly(ethylene glycol)-*block*-poly(propylene glycol)-*block*-poly(ethylene glycol), $EO_{20}PO_{70}EO_{20}$, M_{av} = 5800, Aldrich) was dissolved with stirring in 125 g of 1.9 M HCl solution at room temperature. After adding 32.8 mmol of TEOS (99+%, Aldrich), the resultant solution was equilibrated for 3 h for prehydrolysis, and then 8.2 mmol of MPTMS (95%, Aldrich) and 73.8 mmol of H_2O_2 (30 wt %, Aldrich) were added to the solution. The resulting mixture was stirred at 313 K for 20 h and then transferred into a polypropylene bottle for aging an additional 24 h at 373 K under static conditions. The solid product was obtained by filtration and dried in ambient atmosphere overnight. The template was removed from the as-synthesized material by refluxing in ethanol for 24 h (1.5 g of as-synthesized material per 400 mL of ethanol), filtering, washing with separate portions of water and ethanol, and drying at 333 K, yielding the extracted sulfonic acid-functionalized SBA-15 material.[13a]

The X-ray powder diffraction (XRD) pattern of the sample showed d_{100} = 74 Å and a small (200) peak, shown in Figure 1, indicating that mesoporous silica with channels of 74 Å diameter was synthesized, which has a two-dimensional *p*6*mm* hexagonal symmetry with a well-ordered hexagonal array and one-dimensional channel structure.[13] The XRD data are in agreement with those reported by other authors for samples prepared under similar conditions.[13a]

High-resolution X-ray photoelectron spectroscopy (HR-XPS) analyses of the extracted sulfonic acid-functionalized SBA-15 material were carried out at 5×10^{-9} Torr using the Scienta ESCA-300 photoelectron spectrometer at Lehigh University.[15] The S2p, O1s, Si2p, Si2s, and C1s spectral regions were recorded with 150 eV pass energy, an incremental step size of 0.05 eV and a 0.8 mm slit width. Figure 2a shows the survey spectrum of the catalyst. The $S2p_{3/2}$ binding energy at 168.8 eV was used as an internal standard for all peak positions.[16] Figure 2b shows the curve fitting of S2p binding energies for sulfur species S_I at 169 eV and S_{II} at approximately 164 eV. The higher S2p binding energies (S_I) corresponded to oxidized sulfur in an anchored $\equiv Si(CH_2)_3SO_3H$ species ($\equiv$Si represents Si bonded to three framework atoms), and the lower S2p binding energies (S_{II}) are assigned to sulfur remaining in the original state, i.e., in unoxidized $\equiv Si(CH_2)_3SH$.[16,17] The C1s binding energy was observed at 284.27 eV. The O1s binding energy was found at 532.08 eV, and the Si2p binding energy at 102.75 eV resulted from an overlap of $Si2p_{3/2}$ and $Si2p_{1/2}$ binding

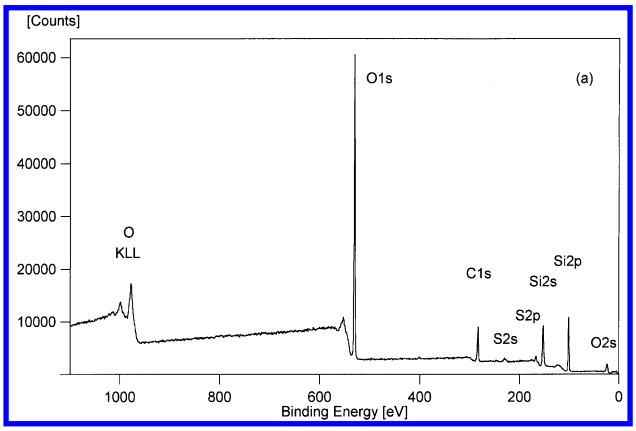

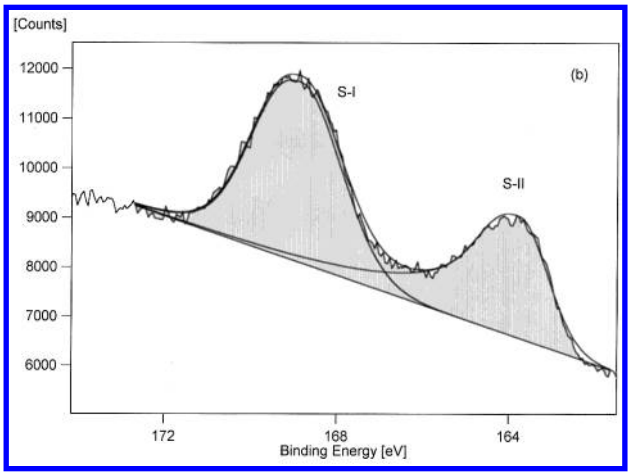

Figure 2. (a) XPS of the extracted propanesulfonic acid-derivatized SBA-15. (b) Curve-fitting of S2p XPS binding energy peaks for the SBA-15 catalyst.

energies. The sulfur ratio between $\equiv Si(CH_2)_3SH$ and $\equiv Si(CH_2)_3SO_3H$ species was calculated to be 0.5/1.0, suggesting two-thirds of the initial $\equiv Si(CH_2)_3SH$ groups were oxidized to alkanesulfonic acid groups bonded onto the mesoporous silica.

The extracted sulfonic acid-functionlized SBA-15 material had a BET surface area of 674 m^2/g. The solid acid-titration technique[13a,16c] was used to determine the acid exchange capacity as 1.64 mequiv of H^+/g of SiO_2, and the unpromoted silica exhibited no acid exchange capacity using the same titration condition. Unlike in base-synthesized MCM-41, after the surfactant was removed by ethanol wash under reflux, the alkanesulfonic acid groups ($R-SO_3H$) remained inside the mesoporous structure of this material.

The dehydrative coupling of methanol (99.8%, anhydrous, Aldrich) with isobutanol (2-methyl-1-propanol, 99.9+%, Alfa) was investigated using 1 g of the extracted sulfonic acid-functionalized SBA-15 catalyst charged into a downflow 0.5-in.-O.D. stainless steel tubular reactor, diluted with 3 mm Pyrex beads. The catalytic reaction was performed in the temperature range 388−523 K, total pressure of 101.3 to 4.2×10^3 kPa (1 atm = 101.325 kPa) and MeOH/*i*-BuOH = 1−2 molar ratio with a carrier gas of 4.94% N_2 diluted in He.[9,10] Steady-state activities were reached within 2 h of the initial alcohol injection or after altering reaction variables such as temperature or pressure. The catalytic testing of the extracted sulfonic acid-functionalized SBA-15 under each condition was carried out for 8−12 h, wherein carbon and oxygen balances were within ±0.2% and no deactivation was observed in long term tests of several hundred hours. The rate of product formation increased with increasing temperature, but the selectivity in favor of

TABLE 1: Product Space Time Yields [(mol/kg of cat)/h] in the Reaction of MeOH/*i*-BuOH (1:1) with Flow Rates of 3.44 (mol/kg of cat)/h Alcohols and 16 (mol/kg of cat)/h Carrier Gas at 101.3 kPa Total Pressure of Carrier Gas and Alcohols over the Extracted Sulfonic Acid-Functionalized SBA-15 Material (Comparisons with Other Previously Studied Catalysts Given)

T/K	MIBE	DME	MTBE	butenes[a]	ethers selectivity (%)
388	0.014	0.006	–[b]	–	100
388[c]	0.058	0.040	–	0.026	79
388[d]	0.082	0.337	0.009	0.218	66
398	0.020	0.009	–	–	100
398[e]	0.011	0.007	0.001	0.028	40
398[f]	0.008	0.008	–	0.008	67
398[g]	0.020	0.006	0.003	0.067	30
423	0.023	0.013	–	0.053	40
448	0.033	0.018	–	0.125	29
473	0.041	0.026	–	0.198	25
498	0.053	0.037	–	0.322	23
523	0.074	0.061	–	0.551	20

[a] Butenes mainly consisted of isobutene but also included *n*-butene and *cis*-and *trans*-2-butene. [b] – indicates "not observed". [c] Nafion-H polymer acid catalyst.[16b] [d] Amberlyst-35 resin catalyst.[10e,16b] [e] SiO_2/Al_2O_3 catalyst.[10c] [f] Montmorillonite catalyst.[10c] [g] ZrO_2/SO_4 catalyst.[10c,16b]

isobutene formation increased rapidly at higher temperature, as presented in Table 1. The methyl isobutyl ether (MIBE) yields of 0.02 (mol/kg of cat)/h at 398 K represented an enhancement of 82−150% over the SiO_2/Al_2O_3 and montmorillonite catalysts.[10c,e] The dimethyl ether (DME) yields of 0.009 (mol/kg of cat)/h increased 50% from 0.006 (mol/kg of cat)/h on SO_4^{2-}/ZrO_2, 29% from 0.007 (mol/kg of cat)/h on the SiO_2/Al_2O_3 catalyst, and 13% from 0.008 (mol/kg of cat)/h on the montmorillonite catalyst.[10c,e] No dibutyl ethers were observed.

Although the extracted sulfonic acid-functionalized SBA-15 material was superior over the inorganic solid acid catalysts in MIBE and DME formation, its catalytic activity was lower than polymer acid catalysts, as shown in Table 1. However, with the present inorganic, high stability catalytic material, the ethers were formed at 100% selectivity below 400 K, which was appreciably higher than observed over either the inorganic catalysts (30−67% selectivity to ethers) or the polymeric acid catalysts (66−79% ether selectivity) previously reported.[10,16b] Further, it is noted that among the ether products, the extracted sulfonic acid-functionalized SBA-15 favored MIBE formation (70% MIBE selectivity at 388 K), whereas the Amberlyst-35 resin catalyst favored DME formation (79% DME selectivity at 388 K in Table 1).

The dehydration of the alcohol mixture (MeOH/*i*-BuOH = 2/1) over the extracted sulfonic acid-functionalized SBA-15 was studied in a wide range of reaction pressures at 388 K. Dramatic increases of MIBE and DME yields were observed with the alcohol pressure. The MIBE product yielded a maximum selectivity of 78% at 80 kPa alcohol partial pressure ($p_M = 54$ kPa, $p_B = 26$ kPa), and DME and MIBE yields approached a constant value above total alcohol partial pressure of about 300 kPa. The effect of pressure was found to be reversible, as observed for the other catalysts previously studied;[10a,b] i.e., when alcohol pressure was decreased to its original value, MIBE and DME decreased to their original rates.

The dehydration reactions are considered to occur to a greater or lesser extent within the catalyst mass, wherein the reactants, products, and solvent are in equilibrium with the gas phase.[18] The kinetic analysis provides an indication that elevated pressure favored the ether-forming reaction in comparison with the dehydration of isobutanol to form butenes, which would correspond to a molar volume increase.[9,10] Figure 3 illustrates

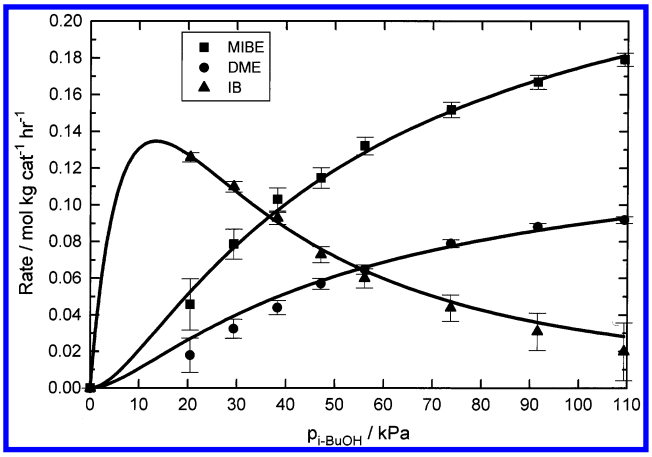

Figure 3. Rates of MIBE formation, ν_{MIBE} (■), DME formation, ν_{DME} (●), and isobutene (IB) formation, ν_{IB} (▲), in the reaction of MeOH/*i*-BuOH (2:1 molar ratio) with flow rates of 15.6 (mol/kg of cat)/h alcohols and 186 (mol/kg of cat)/h carrier gas at 388 K as a function of isobutanol partial pressure, P_{i-BuOH}, are given as data points. The fitted kinetic laws (cf. text) are shown as the curves, giving DME kinetic constant $k_1 = 0.59$ (mol/kg of cat)/h, isobutene kinetic constant $k_3 = 1.79$ (mol/kg of cat)/h, MIBE kinetic constant $k_4 = 1.12$ (mol/kg of cat)/h, methanol adsorption equilibrium constant $K_M = 0.0092$ kPa^{-1}, and isobutanol adsorption equilibrium constant $K_B = 0.019$ kPa^{-1}. Error bars, $0.02(v_{i,max})^2/v_i$, are based on an estimate of 2% error associated with the highest rate measured.

the rate of MIBE formation, ν_{MIBE} (■), DME formation, ν_{DME} (●), and isobutene formation, ν_{IB} (▲), in the reaction of MeOH/*i*-BuOH (2:1 molar ratio) with 15.6 (mol/kg of cat)/h alcohols and 186 (mol/kg of cat)/h carrier gas at 388 K as a function of isobutanol partial pressure, P_{i-BuOH}. The experimental data are indicated as individual points, and the full lines fitting the MIBE and DME data points were obtained using the Langmuir−Hinshelwood kinetic laws[9,10] $\nu_{MIBE} = k_4K_Mp_MK_Bp_B/(1 + K_Mp_M + K_Bp_B)^2$ and $\nu_{DME} = k_1K_M^2p_M^2/(1 + K_Mp_M + K_Bp_B)^2$, where p is the partial pressure of methanol (M) or isobutanol (B). Here, k_1 and k_4 are the appropriate kinetic constants for DME and MIBE formation, and K_M and K_B denote the adsorption equilibrium constants for methanol and isobutanol. The kinetic laws were derived on the basis of the reactions occurring on dual surface acid sites of the catalyst.[10] Such sites are realized in the SBA-based material by the *n*-propane-α-sulfonic acid groups anchored on the silica walls by the γ-carbon. In the present experiment, the ratio of partial pressures of methanol and isobutanol was kept at a constant value $p_M/p_B = 2$ at the entry of the reactor bed while the total pressure was changed as a kinetic variable. This partial pressure ratio prevailed in the entire reaction zone within the range of conversions studied. A further constraint used was that the values of adsorption equilibrium constants K_M and K_B must be identical for both the DME and MIBE rates of formation. Nonlinear fitting of the observed data was performed using the above rate equations for DME and MIBE with weighting factors $0.02(v_{max})^2/v_i$ for each *i*th data point, based on an estimate of a 2% error associated with the highest rates. Values of $K_M = 0.0092 \pm 0.001$ kPa^{-1}, $K_B = 0.019 \pm 0.002$ kPa^{-1}, $k_1 = 0.59 \pm 0.01$ (mol/kg of cat)/h, and $k_4 = 1.12 \pm 0.01$ (mol/kg of cat)/h were obtained. The relative magnitudes of $K_B > K_M$ agreed with those previously observed with other catalysts.[9,10]

In addition, the rate of isobutene formation, represented in Figure 3 as ν_{IB} (▲), was found to obey the kinetic law $\nu_{IB} = k_3K_Bp_B/(1 + K_Mp_M + K_Bp_B)^3$, yielding $k_3 = 1.79 \pm 0.02$ (mol/kg of cat)/h with the same values of K_M and K_B, previously determined from the DME and MIBE data. Hence, the overall

error in the kinetic constants was on the order of ±2% and in the adsorption equilibrium constants, ±11%. Solid curves in Figure 3 represent the theoretical values with $K_M = 0.0092$ kPa^{-1}, $K_B = 0.019$ kPa^{-1}, $k_1 = 0.59$ (mol/kg of cat)/h, $k_3 = 1.79$ (mol/kg of cat)/h, and $k_4 = 1.12$ (mol/kg of cat)/h. These values, however, need a refinement as a larger set of data becomes available. Nevertheless, the main features of the kinetic observations strongly indicate that the present SBA−propanesulfonic acid catalyst performs in a fashion similar to all the inorganic and polymeric solid acid materials studied earlier:[9,10] the selectivity to ethers increases with total pressure, isobutene formation is favored at low pressures, and MTBE is not observed while it is a minor product over other catalysts. The data for isobutene formation over the present SBA-based material show, however, a stronger retardation with isobutanol pressure than previously observed, e.g., with the Nafion-H catalyst.[10b] This feature gives rise to a higher selectivity to ethers over the SBA−propanesulfonic catalyst than on any other solid acid catalyst so far studied. In contrast, sulfated zirconia catalysts favors the formation of isobutene over MIBE and DME.[10c] *Therefore, a large class of solid acid catalysts for dehydrocondensation and dehydration of methanol/isobutanol mixtures has been found to obey similar kinetic laws, while selectivity to MIBE, DME, MTBE, and isobutene is controlled by the total pressure and subtle variations of the surface rate and adsorption equilibrium constants.*

The experimental data also exhibited increasing isobutene yields with increasing temperature (Table 1). The isobutanol dehydration to isobutene competed with MeOH/*i*-BuOH coupling and MeOH dehydration in the reaction system. The enhancement of selectivity for isobutene from 0% at 398 K to 80% at 523 K is in agreement with earlier observations on a large number of solid acid catalysts. The temperature dependence of the rate of formation of the products in Table 1 is determined by a complex combination of the activation energies of the kinetic constants and adsorption enthalpies of the reactants. Nevertheless, the trends are such that the rates are increasing with temperature, for butenes more than the ethers, and MTBE is a very minor or not observed product. In Table 1 we also compare the rates of formation of MIBE, DME, and IB over the present sulfonic acid-derivatized SBA-15 material and earlier studied inorganic and polymeric solid acid catalysts. A remarkable feature of the SBA catalyst is the superior selectivity for ethers at low synthesis temperatures (<400 K).

In summary, the results demonstrate that direct synthesis of sulfonic acid-functionalized mesoporous silica material was successful, resulting in a catalyst possessing hexagonal mesostructure with ∼74 Å pore size, acid exchange capacities of 1.6 mequiv of H^+/g of SiO_2, surface area of 674 m^2/g, and excellent thermal stabilities. Such sulfonic acid groups bonded onto mesoporous silica effectively catalyzed the alcohol coupling reaction forming MIBE and DME at high pressure. The material exhibited high ether selectivities and higher catalytic activity for ether formation than other inorganic solid acid catalysts.

Acknowledgment. We gratefully acknowledge the support of this work by the U.S. Department of Energy (DE-FG02-01ER15181). We thank Dr. John B. Higgins of Air Products and Chemicals, Inc. for the XRD analyses and Dr. Alfred C. Miller for professional and technical assistance with the XPS analyses using the Scienta ESCA facility of Lehigh University.

References and Notes

(1) (a) Bosch, E.; Huber, S.; Weitkamp, J.; Knözinger, H. *Phys. Chem. Chem. Phys.* **1999**, *1*, 579. (b) Grey, C. P.; Poshni, F. I.; Gualtieri, A. F.; Norby, P.; Hanson, J. C.; Corbin, D. R. *J. Am. Chem. Soc.* **1997**, *119*, 1981.

(2) Ramamurthy, V.; Lakshminarasimhan, P.; Grey, C. P.; Johnston, L. J. *J. Chem. Soc., Chem. Commun*. **1998**, 2411.

(3) (a) Shen, G. C.; Liu, A. M.; Ichikawa, M. *Inorg. Chem*. **1998**, *37*, 497. (b) Shen, G. C.; Liu, A. M.; Ichikawa, M. *J. Chem. Soc., Faraday Trans.* **1998,** *96*, 754. (c) Chu, P.-J.; Gerstein, B. C.; Nunan, J.; Klier, K. *J. Phys. Chem*. **1987**, *91*, 3588. (d) Sheu, L. L.; Knözinger, H. K.; Sachtler, W. M. H. *J. Am. Chem. Soc.* **1989**, *111*, 8125.

(4) (a) Shen J. G. C. *J. Phys. Chem. B.* **2001**, *105*, 2336. (b) Shen, J. G. C.; Ichikawa, M. *J. Chem. Phys.* **1999**, *110*, 5933. (c) Shen, G. C.; Shido, T.; Ichikawa, M. *J. Phys. Chem*. **1996**, *100*, 16947.

(5) (a) Klier, K. *Langmuir* **1988**, *4*, 13. (b) Maschmeyer, T.; Rey, F.; Sankar, G.; Thomas, J. M. *Nature* **1995**, *378*, 159. (c) Morey, M. S.; O'Brien, S.; Schwarz, S.; Stucky, G. D. *Chem. Mater*. **2000**, *12*, 898.

(6) (a) Shen J. G. C. *J. Phys. Chem. B* **2000**, *104*, 423. (b) Tanev, P. T.; Chibwe, M.; Pinnavaia, T. J. *Nature* **1994**, *368*, 321.

(7) (a) Shen, J. G. C.; Ichikawa, M. *J. Phys. Chem. B* **1998**, *102*, 5602. (b) Shen, J. G. C.; Liu, A. M.; Tanaka, T.; Ichikawa, M. *J. Phys. Chem. B* **1998**, *102*, 7782. (c) Shen G. C.; Ichikawa, M. *J. Chem. Soc., Faraday Trans.* **1998**, *96*, 754.

(8) Sun, Q.; Herman, R. G.; Klier, K. *J. Chem. Soc., Chem. Commun*. **1995**, 1849.

(9) Shen, J. G. C.; Kalantar, T. H.; Ma, Q.; Herman, R. G.; Klier, K. *J. Chem. Soc., Chem. Commun*. **2001**, 653.

(10) (a) Nunan, J.; Klier, K.; Herman, R. G. *J. Chem. Soc., Chem. Commun*. **1985**, 676. (b) Nunan, J. G.; Klier, K.; Herman, R. G. *J. Catal*. **1993**, *139*, 406. (c) Klier, K.; Herman, R. G.; Johansson, M. A.; Feeley, O. C. *Prepr. Paper (Am. Chem. Soc., Div. Fuel Chem.)* **1992**, *37* (1), 236. (d) Klier, K.; Kwon, H.-H.; Herman, R. G.; Hunsicker, R. A.; Ma, Q.; Bollinger, S. J. In *12th International Congress on Catalysis*; Corma, A., Melo, F. V., Mendioroz, A., Fierro, F. L. S., Eds.; Elsevier: Amsterdam, 2000; p 3447. (e) Klier, K.; Herman, R. G. *Final Technical Report to U.S. Department of Energy (DOE/FC/90044-F)*; U.S. DOE: Washington, DC, 1994; 167 pp. (f) Lietti, L.; Sun, Q.; Herman, R. G. Klier, K. *Catal. Today* **1996**, *27*, 151.

(11) (a) Kresge, C. T.; Leonowicz, M. E.; Roth, W. J.; Vartuli, J. C.; Beck, J. S. *Nature* **1992**, *359*, 710. (b) Beck, J. S.; Vartuli, J. C.; Roth, W. J.; Leonowicz, M. E.; Kresge, C. T.; Schmitt, K. D.; Chu, C. T. W.; Olson, D. H.; Sheppard, E. W.; McCullen, S. B.; Higgins, J. B.; Schlenker, J. L. *J. Am. Chem. Soc*. **1992**, *114*, 10834. (c) Yong, H.; Kuperman, A.; Coombs, N.; Mamiche-Afara, S.; Ozin, G. A. *Nature* **1996**, *379*, 703.

(12) (a) Huo, Q.; Leon, R.; Petroff, P. M.; Stucky, G. D. *Science* **1995**, *268*, 1324. (b) Schacht, S.; Huo, Q.; Voigt-Martin, I. G.; Stucky, G. D.; Schüth, F. *Science* **1996**, *273*. 768. (c) Tanev, P. T.; Pinnavaia, T. J. *Science* **1995**, *267*, 865. (d) Tanev, P. T.; Pinnavaia, T. J.; *Science* **1996**, *271*, 1267. (e) Attard, G. S.; Glyde, J. C.; Göltner, C. G. *Nature* **1995**, *378*, 366.

(13) (a) Margolese, D.; Melero, J. A.; Christiansen, S. C.; Chmelka, B. F.; Stucky, G. D. *Chem. Mater*. **2000**, *12*, 2448. (b) Zhao, D.; Huo, Q.; Feng, J.; Chmelka, B. F.; Stucky, G. D. *J. Am. Chem. Soc*. **1998**, *120*, 6024. (c) Zhao, D.; Feng, J.; Huo, Q.; Melosh, N.; Fredrickson, G. H.; Chmelka, B. F.; Stucky, G. D. *Science* **1998**, *279*, 548.

(14) (a) Van Rhijn, W. M.; De Vos, D. E.; Sels, B. F.; Bossaert, W. D.; Jacobs, P. *J. Chem. Soc., Chem. Commun*. **1998**, 317. (b) Lim, M. H.; Blanford, C. F.; Stein, A. *Chem. Mater*. **1998**, *10*, 467.

(15) Chaney, R. L.; Simmons, G. W. *R&D Magazine* **1990**, *83(9)*, 1.

(16) (a) Johansson, M.; Klier, K. *Top. Catal*. **1997**, *4*, 99. (b) Johansson, M. Ph.D. Dissertation, Lehigh University, Bethlehem, PA, 1995. (c) Shen, J. G. C.; Kalantar, T. H.; Herman, R. G.; Roberts, J. E.; Klier, K. *Chem. Mater*. **2001**, *13*, 4479.

(17) Moulder, J. F.; Stickle, W. F.; Sobul, P. E.; Bomben, K. D. *Handbook of X-ray Photoelectron Spectroscopy*; Chastain, J., Ed.; Perkin-Elmer Corp.: Eden Prairie, MN, 1992.

(18) (a) Polanskii, N. G.; *Russ. Chem. Rev*. **1974**, *39*, 244. (b) Helfferich, F. *J. Am. Chem. Soc*. **1954**, *76*, 5567.